# Double-Pole Approximation in Time-Dependent Density Functional Theory

H. Appel and E.K.U. Gross

*Fachbereich Physik, Freie Universität Berlin,*

*Arnimallee 14, D-14195 Berlin-Dahlem, Germany.*

K. Burke

*Department of Chemistry and Chemical Biology,*

*Rutgers University, 610 Taylor Rd, Piscataway, NJ 08854*

(Dated: January 3, 2006)

## Abstract

A simple approximate solution to the linear response equations of time-dependent density functional theory (TDDFT) is given. This extends the single-pole approximation (SPA) to two strongly-coupled poles. The analysis provides both an illustration of how TDDFT works when strong exchange-correlation effects are present and insight into such corrections. For example, interaction can cause a transition to vanish entirely from the optical spectrum.

## INTRODUCTION

Ground-state density functional theory (DFT) has been very successful for atoms, molecules, and solids [1, 2]. Similar success is now being enjoyed by time-dependent DFT (TDDFT) [3, 4], because of its combination of accuracy combined with low computational cost [5]. While TDDFT has a huge variety of applications [6], it is low-lying photo-excitations of molecules that has seen its greatest use [5].

In the present work, we restrict our discussion to linear response of a non-degenerate ground-state. Just as in ground-state DFT, all many-body effects, i.e., exchange and correlation (XC), are contained in a well-defined functional, the XC kernel [7]. In any practical calculation, this functional must be approximated. In most calculations, an adiabatic approximation is made, and the static limit of the kernel is applied. Typical approximations are then adiabatic local density approximation (ALDA) [7] or generalized gradient approximation, or exact exchange [8–10]. The reliability and accuracy of these approximations to TDDFT is much less well-understood than it is in ground-state DFT.

One can do many calculations on many systems, in order to gain insight into the accuracy and reliability of theory, but it can be much more effective to develop simple approximations to the solution of the TDDFT response problem [11]. A classic example is the single-pole approximation [12], within which TDDFT yields a simple correction to the KS transition frequencies which is just the expectation value of the Hartree-XC kernel on the transition orbitals. While usually accurate [11], the most important feature of this approximation is the insight it yields into the workings of TDDFT. It yields a first approximation to TDDFT effects with almost no extra effort beyond a ground-state calculation, and gives a simple picture for such effects [13]. It has also been shown [11] that, if a transition is only weakly-coupled to others in the system, one can use this to estimate the XC kernel itself. Unfortunately, this is rarely the case in practice.

In the present work, we generalize the SPA to a *double-pole* approximation (DPA), in which we explicitly solve the TDDFT response equations for exactly two transitions. This produces a variety of results beyond that of SPA. Most importantly, one can study TDDFT XC corrections to KS levels when there is strong coupling between levels. But one can also see when SPA fails, and recover Görling-Levy perturbation theory [14] results for the coupling-constant expansion of excited states [11]. DPA has recently been successfully applied to

core-hole interaction in the X-ray absorption spectroscopy of 3d transition metals [15].

## DOUBLE-POLE APPROXIMATION

In the matrix-formulation of the TDDFT response equation within the adiabatic approximation, the exact eigenvalues and oscillator strengths can be obtained from the solution of the following eigenvalue problem [16]

$$\sum_{q'} W_{qq'}(\Omega)\ v_{q'} = \Omega^2\ v_q, \tag{1}$$

where the matrix $W$ is given by

$$W_{qq'}(\Omega) = \omega_q^2\,\delta_{qq'} + 4\,\sqrt{\omega_q\,\omega_{q'}}\,M_{qq'}(\Omega) \tag{2}$$

and

$$M_{qq'}(\Omega) = \int d^3r \int d^3r'\,\Phi_q^*(\mathbf{r})\,K(\mathbf{r}\mathbf{r}'\Omega)\,\Phi_{q'}(\mathbf{r}'). \tag{3}$$

Here $\omega_i$ is the Kohn-Sham transition frequency and for single particle transitions $q$ ($q \equiv k \rightarrow j$) the shorthand $\Phi_q(\mathbf{r}) := \varphi_k(\mathbf{r})\varphi_j^*(\mathbf{r})$ has been introduced. The kernel $K(\mathbf{r}, \mathbf{r}\,', \omega)$ consists of the bare Coulomb interaction and the approximate XC kernel $f_{\rm XC}(\mathbf{r}, \mathbf{r}', \omega)$:

$$K(\mathbf{r}, \mathbf{r}', \omega) = \frac{1}{|\mathbf{r} - \mathbf{r}'|} + f_{\rm XC}(\mathbf{r}, \mathbf{r}', \omega). \tag{4}$$

Atomic units ($e^2 = \hbar = m = 1$) are used throughout.

We now solve these equations exactly for a $2\times2$-system, i.e., ignoring coupling to all other transitions. To simplify the discussion we assume a frequency independent kernel and real orbitals, i.e. $M_{qq'} = M_{q'q}$. Thus the relation between matrix elements of Casida's equation and the kernel is:

$$W_{ii} = \omega_i^2 + 4\,\omega_i\,M_{ii}, \qquad W_{12} = 4\,\sqrt{\omega_1\omega_2}\,M_{12}. \tag{5}$$

Next define the average

$$\overline{W} = \frac{1}{2}\,(W_{11} + W_{22}) \tag{6}$$

and difference

$$\Delta W = W_{22} - W_{11} \tag{7}$$

of the diagonal elements. We define a mixing angle by:

$$\tan\theta = \frac{2\,W_{12}}{\Delta W}, \tag{8}$$

choosing the branch between 0 and $\pi$. The eigenvalues can then be written succinctly as

$$\Omega_{\pm}^2 = \overline{W} \pm \frac{1}{2}\frac{\Delta W}{\cos\theta}, \tag{9}$$

while the *normalized* eigenvectors are

$$\vec{v}_+ = \begin{pmatrix} \sin\frac{\theta}{2} \\ \\ \cos\frac{\theta}{2} \end{pmatrix}, \qquad \vec{v}_- = \begin{pmatrix} -\cos\frac{\theta}{2} \\ \\ \sin\frac{\theta}{2} \end{pmatrix}. \tag{10}$$

The physical oscillator strength can be obtained from the following expression [16]

$$f_{\pm} = \frac{2}{3}\,|\vec{x}^T\, S^{-\frac{1}{2}}\,\vec{v}_{\pm}|^2, \tag{11}$$

where

$$S^{-\frac{1}{2}} = \begin{pmatrix} \sqrt{\omega_1} & 0 \\ \\ 0 & \sqrt{\omega_2} \end{pmatrix}, \qquad \vec{x} = \begin{pmatrix} x_1^{KS} \\ \\ x_2^{KS} \end{pmatrix}, \tag{12}$$

and the $x_j^{KS}$ denote dipole matrix elements of KS orbitals. Given that there are only two transitions, we give a geometric meaning to the oscillator strengths. Writing

$$f_1^{\mathrm{KS}} = \sin^2\alpha^{\mathrm{KS}}, \qquad f_2^{\mathrm{KS}} = \cos^2\alpha^{\mathrm{KS}} \tag{13}$$

and

$$f_- = \sin^2\alpha, \qquad f_+ = \cos^2\alpha, \tag{14}$$

we find

$$\alpha = \alpha^{\mathrm{KS}} - \theta/2, \tag{15}$$

i.e., the oscillator strengths are represented by a unit vector in 2d space, and the coupling merely rotates this vector. Note that the Thomas-Reiche-Kuhn (TRK) sum rule (sum of the oscillator strengths is 1) is obviously preserved.

## SINGLE-POLE APPROXIMATION

As mentioned above, the single-pole approximation is a useful approximation to TDDFT results. We recover SPA results by inserting $\theta = 0$ in our formulas. Thus

$$\Omega_{\pm}^{\mathrm{SPA}} = \sqrt{\overline{W} \pm \frac{\Delta W}{2}} \tag{16}$$

and the oscillator strengths reduce to their KS values.

We can now study the leading corrections to SPA produced by DPA when the coupling between poles is weak. Writing $\eta = W_{12}/\Delta W$, and assuming $\eta << 1$, for the eigenvalues, we find

$$\Omega\pm = \Omega_{\pm}^{\rm SPA} \pm \frac{W_{12}}{2\,\Omega_{\pm}^{\rm SPA}}\eta + O(\eta^2), \tag{17}$$

while for the oscillator strengths, we have

$$\begin{aligned} f_+ &= f_2^{KS} + 2\eta\sqrt{f_1^{KS} f_2^{KS}} + O(\eta^2), \\ f_- &= f_1^{KS} - 2\eta\sqrt{f_2^{KS} f_1^{KS}} + O(\eta^2). \end{aligned} \tag{18}$$

Note that the corrections to the peak positions are second-order in $W_{12}$, while the corrections to $\sqrt{f_\pm}$ are first-order. Thus SPA is expected to be much better for peak positions than for peak heights.

Lastly, we point out that this expansion was deduced for the general case in Ref. [11], and used (among other things) to identify coefficients in the Görling-Levy expansion of excited-state energies. Our results here agree with those, but in the special case of transitions to which DPA applies, yield results that include a resummation of *all* orders in the adiabatic coupling constant of density functional theory.

## HIGH-FREQUENCY LIMIT

So far we have given exact results for the double-pole approximation. However, in many cases where DPA applies, there is a further simplification. Usually the two transitions are closer to each other than any others that couple to the pair. If in addition their frequency difference is small relative to their mean frequency, for both the interacting and KS systems, i.e.,

$$\overline{\Omega},\, \overline{\omega} >> \Delta\Omega,\, \Delta\omega, \tag{19}$$

we find much simpler results, which are very useful for interpretation.

The SPA discussed above reduces to

$$\Omega_{\pm}^{\rm SPA} = \omega_i + 2\,M_{ii}, \qquad (i = 1, 2). \tag{20}$$

In fact, the original SPA was applied for just a forward transition, yielding exactly this result [12]. In general the symmetric result (sometimes called the small-matrix approximation

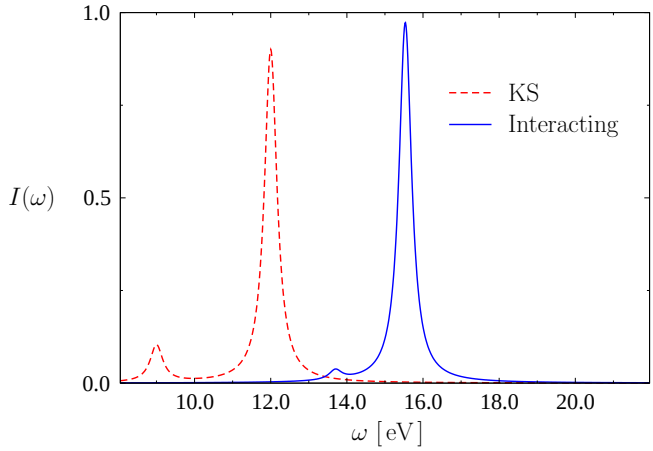


FIG. 1: Interacting and Kohn-Sham spectra as function of frequency ($\omega_1 = 9$ eV, $M_{12} = 0.2$ eV).

[17, 18]) is preferable. We use the term SPA to mean the symmetric result throughout this paper.

The mixing angle is given by

$$\tan\theta = \frac{4M_{12}}{\Delta\Omega^{\rm SPA}}, \tag{21}$$

i.e., it is the ratio of the off-diagonal matrix elements of the kernel on the scale of the separation in SPA that matters. We find

$$\Omega_\pm = \overline{\Omega^{\rm SPA}} \pm \frac{\Delta\Omega^{\rm SPA}}{2\cos\theta}. \tag{22}$$

SPA yields the correct average position of the two lines, but their splitting is greater than SPA predicts (level repulsion).

## ILLUSTRATIONS

To illustrate our results, consider a weak lower-frequency transition ($\omega_1 = 9$ eV, $f_1^{KS} = 1/10$) and a strong higher-frequency transition ($\omega_2 = 12$ eV, $f_2^{KS} = 9/10$). We imagine these have significant diagonal kernel matrix elements $M_{11} = 3$ eV, $M_{22} = 2$ eV, but are not strongly coupled to one another, $M_{12} = 0.2$ eV. We have plotted the interacting and KS spectra in Fig. 1. The peaks are Lorentzians of width 0.2, mimicking a measurement of

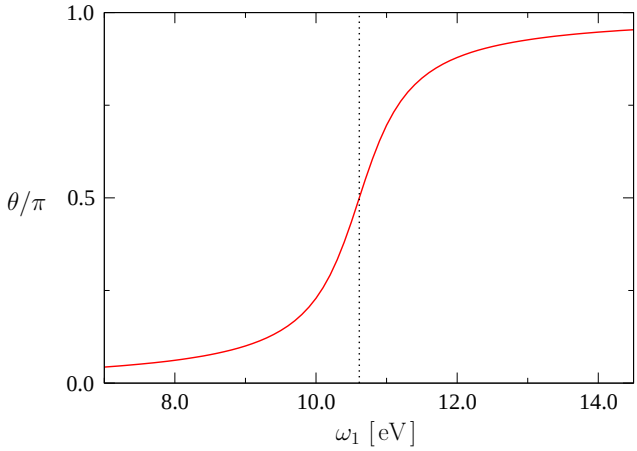


FIG. 2: The scaled coupling angle $\theta/\pi$ as function of the position of the lower transition.

finite resolution. Because the coupling is weak, the single-pole approximation is excellent, and accurately predicts the large shifts in positions. However, SPA wrongly predicts no variation in oscillator strength. In fact, one can see from the figure that the first peak has actually *lost* intensity relative to its KS value.

In the rest of this section, we explore what happens in the DPA model of TDDFT. In order to emphasize that it is not the absolute magnitude of the off-diagonal matrix element that is significant, but rather its strength relative to the separation between the peaks, we now consider all the same parameters, but imagine increasing $\omega_1$. In Fig. 2, we plot the mixing angle as a function of $\omega_1$. At $\omega_c = 2\,(-3+\sqrt{69})$ eV $\approx 10.61$ eV, the diagonal matrix elements $W_{ii}$ match, so that $\Delta W = 0$ and $\theta = \pi/2$. At that point, the peaks are a 50:50 mixture of the two KS levels. In that region, the levels are strongly coupled, and the spectrum distorts mightily from its KS shape. The width of the transition region can be defined as the change in frequency needed to bring $\theta$ from $\pi/4$ to $3\pi/4$, and, from Eq. (21) in the high-frequency limit, is seen to be $4M_{12} = 0.8$ eV here, i.e., proportional to the off-diagonal element, but quite a bit larger. More significantly, there are tails in the transition that decay extremely slowly with pole separation. On the contrary, SPA yields a function that steps from 0 to 1 at $\omega_c$.

To see this, in Fig. 3, we plot the interacting levels $\Omega_\pm$ as a function of $\omega_1$, and observe the avoided crossing. Note that straight line plots, extrapolated from the limits where $\omega_1$ is either far above or far below $\omega_c$, yield extremely accurate results almost everywhere. This is the SPA result. In fact, from Eqs. (9) and (16), we see that the crossover point is *exactly*

given by SPA. Moreover, in the high-frequency limit, Eqns. (20)-(22) yield

$$|\Delta\Omega|^2 = |\Delta\Omega^{\rm SPA}|^2 + 16\,|M_{12}|^2. \tag{23}$$

So if the off-diagonal matrix elements are small relative to the SPA separation, the true separation is not much greater; the closest the two levels come is a separation of $4\,|M_{12}|$, i.e., they never cross.

But in Fig. 4, we plot the associated oscillator strengths. The effect of coupling is extremely dramatic. Note first that, for $\omega_1$ below the strong coupling region, the bigger peak is *enhanced* above its KS value, and the smaller one reduced. This is pole repulsion, and it is felt even very far from the strong coupling region. This effect is entirely missing from SPA. Next we see that there is even a critical value $\omega_d$ ($d$ for *dark*) at which $f_- = 0$ exactly. This means the lower peak disappears entirely, and all strength is in the upper peak (Fig. 5)! From Eqs. (15) and (21), we find

$$\Delta\Omega^{\rm SPA} = g(\alpha^{\rm KS})\,|M_{12}| \qquad (f_1 = 0), \tag{24}$$

where $g(\alpha) = 4/\tan 2\alpha = 16/3$ for $f_1^{\rm KS} = 0.1$ as is the case here. This yields 8.93 eV, whereas the exact result is 9.90 eV.

By increasing $\omega_1$ just a little more, we come to the position of the avoided crossing $\omega_c$ ($c$ for *crossing*), where $\theta = \pi/2$. In fact, Eqs. (13)-(15) yield here

$$f_\pm = \frac{1}{2} \pm \langle f^{\rm KS}\rangle, \tag{25}$$

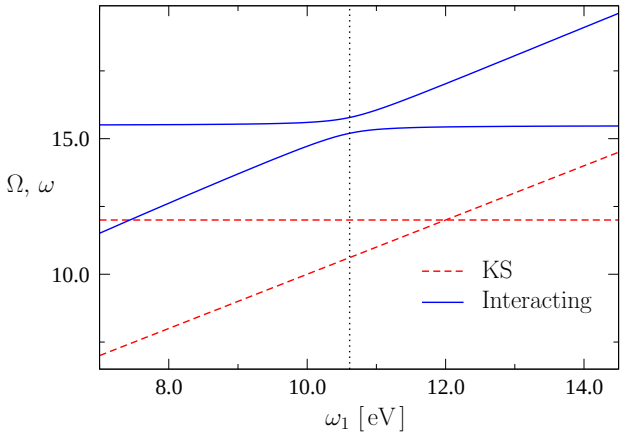


FIG. 3: Interacting and Kohn-Sham excitation energies as function of $\omega_1$.

where $\langle f^{\rm KS}\rangle$ denotes the geometric mean, $\sqrt{f_1^{\rm KS}\, f_2^{\rm KS}}$. In our case, this yields $f_- = 0.2$ and $f_+ = 0.8$, respectively, giving the lower peak *double* its KS weight. In Fig 6, we show the spectrum for $\omega_1 = \omega_c$, and observe how much it differs from its KS doppelganger. There appears to be only one peak, but in fact there are still two, although the broadening obscures this. They are very close together.

The final interesting point is $\omega_e$ ($e$ for *equal*), where the interacting oscillator strengths equal, i.e., both are 1/2. At the equality point, $\alpha = \pi/4$, and so $\theta = \pi/2 - 2\alpha^{\rm KS}$. Again using the high-frequency limit, Eq. (21), yields

$$\Delta\Omega^{\rm SPA} = -4\, M_{12}\cot(2\alpha^{\rm KS}), \tag{26}$$

i.e., the same distance above the crossing point, as the amount the point $f_- = 0$ is below. This yields 12.29 eV, whereas the exact number is 11.02 eV (Fig. 7).

Finally, in Fig. 8, we consider $\omega_1 = 13$ eV. Now the oscillator strengths have returned (almost) to their KS values, but + and − have been reversed. Lastly, we demonstrate the dependence of these results on the strength of $M_{12}$ relative to the diagonal elements. We have so far presented only the case $M_{12} << M_{ii}$. But we have argued that it is only the ratio $|M_{12}|/\Delta\Omega^{\rm SPA}$ that matters. Thus increasing $M_{12}$ does not change the shape of the curves (around the turnover point), but only changes the scale on which the action takes place. In Fig. 9, we change $M_{12}$ to 1 eV and 2.5 eV, and see this occur. Since the turnover occurs on a scale of about $4|M_{12}|$, almost the entire region has strong coupling for $M_{12} = 2.5$ eV.

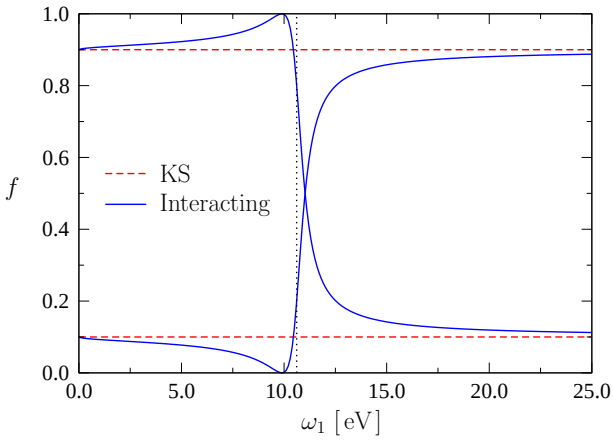


FIG. 4: Oscillator strengths as function of $\omega_1$ .

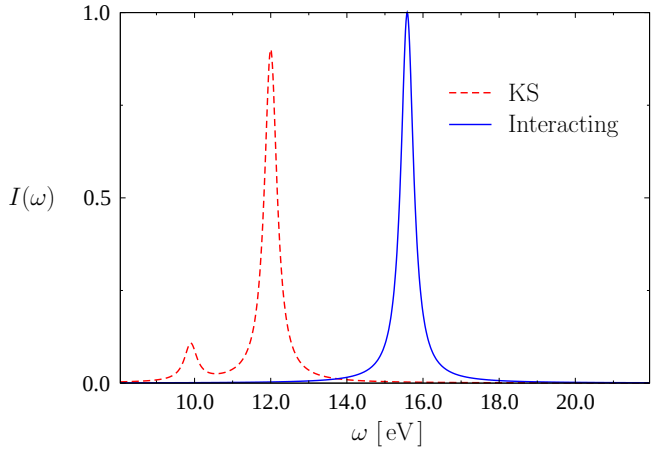


FIG. 5: Interacting and Kohn-Sham spectra at the critical value $\omega_1 = \omega_d \approx 9.90$ eV. All intensity is in the upper transition.

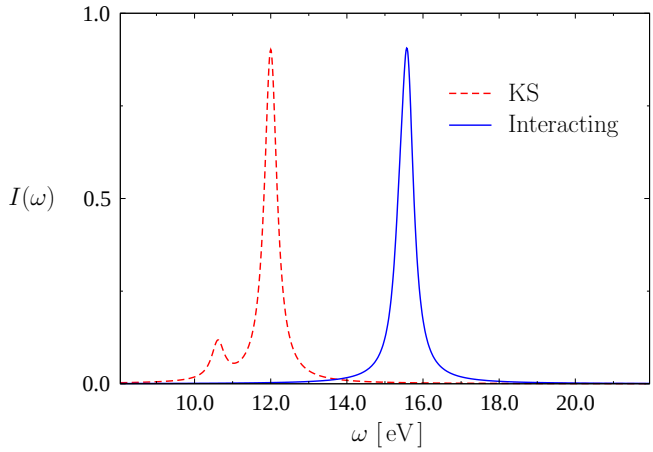


FIG. 6: Interacting and Kohn-Sham spectra for $\omega_1 = \omega_c \approx 10.61$ eV.

Lastly, we examine this behavior as a function of $M_{12}$. In Figs. 10 and 11, we repeat the plot of oscillator strengths versus $\omega_1$ for this system, but now with $M_{12} = 1$ eV and $M_{12} = 2.5$ eV, respectively. We see that the larger values lead to qualitatively similar behavior, but over a broader frequency scale.

## INVERSION

The above sections present the TDDFT response equations in the usual manner. First solve the ground-state KS problem, finding occupied and unoccupied levels, then calculate

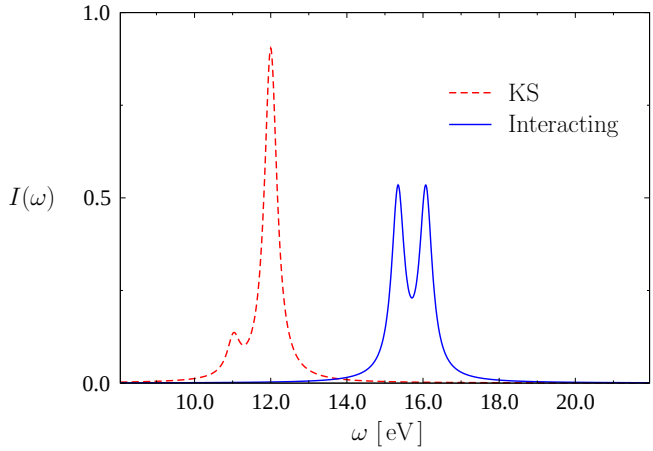


FIG. 7: Interacting and Kohn-Sham spectra for $\omega_1 = \omega_e \approx 11.02$ eV, producing equal interacting oscillator strengths.

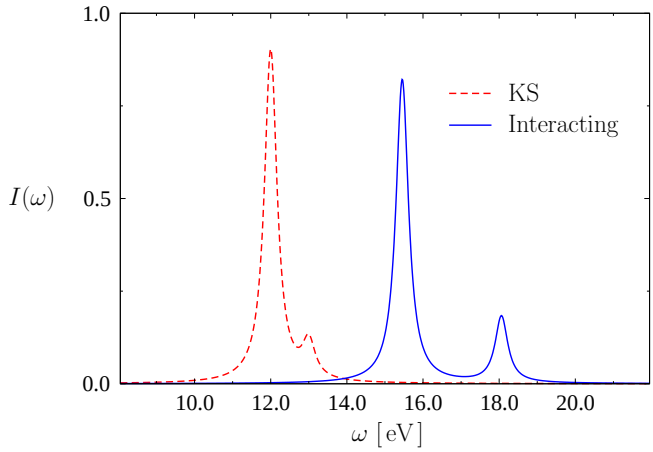


FIG. 8: Interacting and Kohn-Sham spectra for $\omega_1 = 13$ eV.

matrix elements of the kernel (with some functional approximation), and calculate the true transitions and oscillator strengths of your system. However, we are motivated to gain insight into the excitations, and so we ask the reverse question: Given the experimental spectrum, what can we learn about the kernel? Inverting our equations to solve for $\theta$ yields:

$$\theta = 2\,(\alpha - \alpha^{\mathrm{KS}}) \tag{27}$$

Thus, knowledge of the KS oscillator strengths, combined only with the experimental oscillator strengths, yields the mixing angle, which measures how strongly the transitions are mixed! No knowledge of the *positions* of transitions is needed.

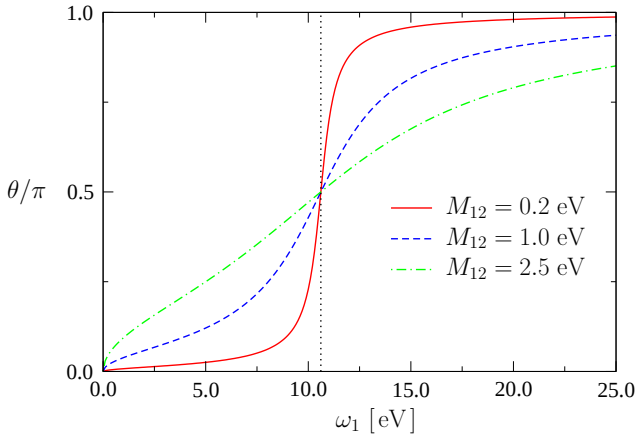


FIG. 9: The scaled coupling angle $\theta/\pi$ as function of $\omega_1$. The plot compares three different regimes for the off-diagonal matrix element $M_{12}$.

Solving for the diagonal matrix elements we arrive at

$$\begin{aligned} W_{11} &= \overline{\Omega^2} - (\Delta\Omega^2/2)\cos\theta, \\ W_{22} &= \overline{\Omega^2} + (\Delta\Omega^2/2)\cos\theta, \end{aligned} \tag{28}$$

where $\overline{\Omega^2}$ is the average of $\Omega^2$ and $\Delta\Omega^2$ is the difference, while the off-diagonal matrix element is

$$W_{12} = (\Delta\Omega^2/2)\ \sin\theta. \tag{29}$$

Again, the experimental positions combined with the mixing angle are sufficient to determine the elements of the matrix $W$. The kernel matrix elements themselves are then found simply,

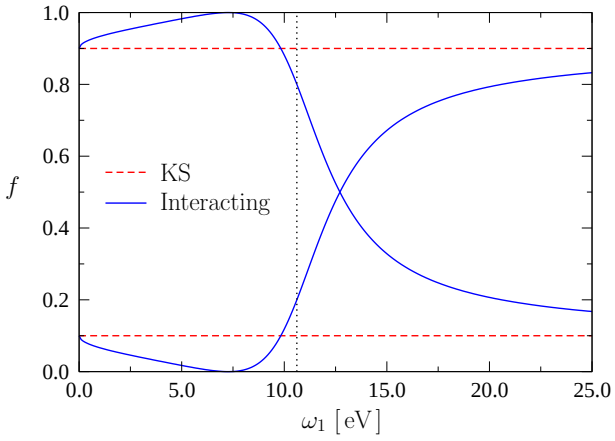


FIG. 10: Same as Fig. 4, but for the case $M_{12} = 1.0$ eV.

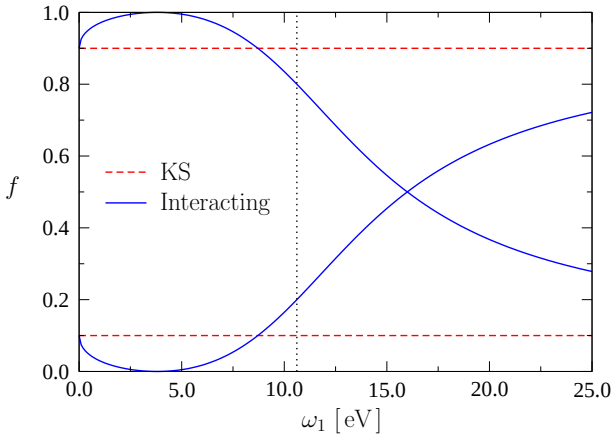


FIG. 11: Same as Fig. 4, but for the case $M_{12} = 2.5$ eV.

by using the KS transition frequencies:

$$M_{jj} = \frac{W_{jj}}{4\,\omega_j} - \frac{\omega_j}{4} \tag{30}$$

and

$$M_{12} = \frac{\Delta\Omega^2\ \sin\theta}{8\sqrt{\omega_1\omega_2}}. \tag{31}$$

These equations provide an exact way to recover the matrix elements $W_{ij}$ of the original matrix and therefore the matrix-elements $M_{ij}$ of the kernel $K$ solely from the knowledge of the eigenvalues and the angle $\theta$.

While the above formulas are completely general, in practice strong coupling tends to occur between neighboring transitions. In those cases, the differences between the two transition frequencies are often much smaller than the transition frequencies themselves. Thus we expand in the small parameter $\Delta\Omega/\overline{\Omega}$, to find

$$\begin{aligned} W_{11} &= \overline{\Omega}\,\left(\overline{\Omega} - \Delta\Omega\ \cos\theta\right), \\ W_{22} &= \overline{\Omega}\,\left(\overline{\Omega} + \Delta\Omega\ \cos\theta\right), \\ W_{12} &= \overline{\Omega}\,\Delta\Omega\ \sin\theta. \end{aligned} \tag{32}$$

To further extract the matrix elements of the kernel, we assume the KS transitions satisfy the same requirement, i.e., that the experimental transitions are close to the KS ones on the scale of the average transition. This yields:

$$M_{11} = (\overline{\Omega} - \Delta\Omega\cos\theta)/4 - \omega_1/4,$$

$$M_{22} = (\overline{\Omega} + \Delta\Omega\cos\theta)/4 - \omega_1/4,$$
$$M_{12} = (\Delta\Omega/4)\sin\theta. \quad (33)$$

These simple expressions give the matrix elements directly, once the KS and experimental information is known. The mixing angle is determined completely by the oscillator strengths, as in Eq. (27). These expressions were used to analyze X-ray absorption spectra in Ref. [15].

## CONCLUSIONS

To summarize, we have presented the exact formulas that arise from a double-pole approximate solution to the TDDFT linear response equations. We have shown how these reduce to the single-pole approximation when the coupling between transitions is weak, and derived the leading terms in this expansion, finding results consistent with those of Ref. [11]. However, with DPA, we can go beyond that work, by considering strong coupling. We also derive simpler expressions that are valid when the transitions are of much higher frequency than the splittings. We illustrated our results, finding (i) that the oscillator strengths can deviate significantly from their KS values, even when the coupling is very weak, (ii) that the scale to compare the off-diagonal matrix element to is the splitting in the single-pole approximation, and (iii) that the weaker peak even vanishes at a special value of the coupling.

KB acknowledges support of the US Department of Energy under grant number DE-FG02-01ER45928, and the National Science Foundation under grant number CHE-0355405. Partial financial support by the EXC!TING Research and Training Network of the EU, the NANOQUANTA network of excellence and the Deutsche Forschungsgemeinschaft within Sfb658 is gratefully acknowledged.

[1] *Self-consistent equations including exchange and correlation effects*, W. Kohn and L.J. Sham, Phys. Rev. **140**, A 1133 (1965).

[2] *A Primer in Density Functional Theory*, ed. C. Fiolhais, F. Nogueira, and M. Marques (Springer-Verlag, NY, 2003).

[3] *Density-functional theory for time-dependent systems*, E. Runge and E.K.U. Gross, Phys. Rev. Lett. **52**, 997 (1984).

[4] *Time-dependent density functional theory: Past, present, and future*, K. Burke, J. Werschnik, and E.K.U. Gross, J. Chem. Phys. **123**, 062206 (2005).

[5] *Density functional methods for excited states: equilibrium structure and excited spectra*, F. Furche and D. Rappoport, to appear in *Computational Photochemistry*, ed. M. Olivucci, Elsevier, Amsterdam, 2005.

[6] *Time-Dependent Density-Functional Theory*, M.A.L. Marques and E.K.U. Gross, Annu. Rev. Phys. Chem. **55**, 427 (2004).

[7] *Local density-functional theory of frequency-dependent linear response*, E.K.U. Gross and W. Kohn, Phys. Rev. Lett. **55**, 2850 (1985); **57**, 923 (1986) (E).

[8] *Time-dependent optimized effective potential*, C.A. Ullrich, U.J. Gossman, and E.K.U. Gross, Phys. Rev. Lett. **74**, 872 (1995).

[9] *Time-dependent optimized effective potential in the linear response regime*, M. Petersilka, U.J. Gossmann, and E.K.U. Gross, in *Electronic Density Functional Theory: Recent Progress and New Directions*, eds. J.F. Dobson, G. Vignale, and M.P. Das (Plenum, NY, 1998).

[10] *Exact exchange-correlation kernel for dynamic response properties and excitation energies in density-functional theory*, A. Görling, Phys. Rev. A, **57**, 3433 (1998).

[11] *Excitations in Time-Dependent Density-Functional Theory*, H. Appel, E.K.U.Gross, and K. Burke, Phys. Rev. Lett. **90**, 043005 (2003).

[12] *Excitation energies from time-dependent density-functional theory*, M. Petersilka, U.J. Gossmann, and E.K.U. Gross, Phys. Rev. Lett. **76**, 1212 (1996).

[13] *Electron-molecule scattering from time-dependent density functional theory*, A. Wasserman, N.T. Maitra, and K. Burke, J. Chem. Phys. **122**, 133103 (2005).

[14] *Correlation-energy functional and its high-density limit obtained from a coupling-constant perturbation expansion*, A. Görling and M. Levy, Phys. Rev. B **47**, 13105 (1993).

[15] *Measuring the kernel of time-dependent density functional theory with X-ray absorption spectroscopy of 3d transition metals*, A. Scherz, E.K.U. Gross, H. Appel, C. Sorg, K. Baberschke, H. Wende, and K. Burke, Phys. Rev. Lett., submitted (2005)

[16] *Time-dependent density functional response theory of molecular systems: Theory, computational methods, and functionals*, M.E. Casida, in *Recent developments and applications in*

*density functional theory*, ed. J.M. Seminario (Elsevier, Amsterdam, 1996).

[17] *Ab Initio Excitation Spectra and Collective Electronic Response in Atoms and Clusters*, I. Vasiliev, S. Ögüt, and J.R. Chelikowsky, Phys. Rev. Lett. **82**, 1919 (1999).

[18] *Molecular excitation energies from time-dependent density functional theory*, T. Grabo, M. Petersilka, and E.K.U. Gross, in J. Mol. Structure (Theochem), **501**, 353 (2000).